

# The Relationship between Plasma Flow Doppler Velocities and Magnetic Field Parameters During the Emergence of Active Regions at the Solar Photospheric Level

A. Khlystova<sup>1</sup>

© Springer ●●●

**Abstract** A statistical study has been carried out of the relationship between plasma flow Doppler velocities and magnetic field parameters during the emergence of active regions at the solar photospheric level with data acquired by the *Michelson Doppler Imager* (MDI) onboard the *Solar and Heliospheric Observatory* (SOHO). We have investigated 224 emerging active regions with different spatial scales and positions on the solar disc. The following relationships for the first hours of the emergence of active regions have been analysed: i) of peak negative Doppler velocities with the position of the emerging active regions on the solar disc; ii) of peak plasma upflow and downflow Doppler velocities with the magnetic flux growth rate and magnetic field strength for the active regions emerging near the solar disc centre (the vertical component of plasma flows); iii) of peak positive and negative Doppler velocities with the magnetic flux growth rate and magnetic field strength for the active regions emerging near the limb (the horizontal component of plasma flows); iv) of the magnetic flux growth rate with the density of emerging magnetic flux; v) of the Doppler velocities and magnetic field parameters for the first hours of the appearance of active regions with the total unsigned magnetic flux at the maximum of their development.

**Keywords:** Active Regions, Magnetic Fields; Active Regions, Velocity Field; Center-Limb Observations

## 1. Introduction

Solar magnetic flux emerges at various spatial scales (*e.g.* Parnell *et al.*, 2009). Golovko (1998) revealed a power-law relation between the maximum magnetic flux and the lifetime of active regions. Otsuji *et al.* (2011) found a relation between the flux growth rate and the maximum magnetic flux in the form of a power-law function.

---

<sup>1</sup> The Institute of Solar-Terrestrial Physics, Siberian Branch,  
Russian Academy of Sciences  
email: khlystova@iszf.irk.ru

Measurements of Doppler velocities indicated that there is a vertical plasma upflow up to  $1 \text{ km s}^{-1}$  at the polarity inversion line when active regions emerge in the solar photosphere (Brants, 1985a; Brants, 1985b; Tarbell *et al.*, 1989; Lites, Skumanich, and Martinez Pillet, 1998; Strous and Zwaan, 1999; Kubo, Shimizu, and Lites, 2003; Guglielmino *et al.*, 2006; Grigor'ev, Ermakova, and Khlystova, 2007; Grigor'ev, Ermakova, and Khlystova, 2009). Grigor'ev, Ermakova, and Khlystova (2007) revealed high Doppler velocities of about  $1.7 \text{ km s}^{-1}$  at the beginning of the emergence of the powerful active region NOAA 10488 at heliographic coordinates N08 E31 ( $B_0+4.9^\circ$ ). The observed Doppler velocities have not been compared with the parameters of the magnetic fields.

The cold and dense plasma contained inside magnetic flux emerging into the solar atmosphere flows down along the magnetic field lines with velocities of up to  $2 \text{ km s}^{-1}$  at the photospheric level (Gopasyuk, 1967; Gopasyuk, 1969; Kawaguchi and Kitai, 1976; Bachmann, 1978; Zwaan, Brants, and Cram, 1985; Brants, 1985a; Brants, 1985b; Brants and Steenbeek, 1985; Lites, Skumanich, and Martinez Pillet, 1998; Solanki *et al.*, 2003; Lagg *et al.*, 2007; Xu, Lagg, and Solanki, 2010). Observations of pores revealed a statistical relation between the Doppler velocity of plasma downflow and the magnetic field strength. Bonaccini *et al.* (1991), studying a large pore, found that the strong magnetic fields correlate linearly with downflow Doppler velocities in the form  $B = 500 V$ , where  $B$  is in Gauss and  $V$  is in  $\text{km s}^{-1}$ . Keil *et al.* (1999) found that downflow Doppler velocities inside pores correlate positively with the magnetic field strength. Cho *et al.* (2010) analysed small pores less than  $2''$ , which were not related to magnetic flux emergence, by using high spatial resolution data from *Hinode*. The authors revealed a negative correlation between positive Doppler velocities and the magnetic field strength, *i.e.* small downflow Doppler velocities corresponded to strong magnetic fields. Grigor'ev, Ermakova, and Khlystova (2011) have shown that in the emerging active region during the formation of pores the plasma downflow Doppler velocity increases linearly with the magnetic field strength.

Estimations of horizontal velocities in the emerging active regions were performed indirectly. A wide range of velocity values from  $0.1$  to  $5.5 \text{ km s}^{-1}$  were obtained by analysing displacements of magnetic field structures (Frazier, 1972; Schoolman, 1973; Harvey and Martin, 1973; Chou and Wang, 1987; Barth and Livi, 1990; Strous and Zwaan, 1999; Hagenaar, 2001; Grigor'ev, Ermakova, and Khlystova, 2009; Otsuji *et al.*, 2011). Considering the separation of opposite polarity poles in 24 bipolar pairs Chou and Wang (1987) found no relation of horizontal velocities neither with the average magnetic field strength nor with the total unsigned magnetic flux. Otsuji *et al.* (2011) studied 101 emerging flux regions with various spatial scales. They showed a power-law relation with negative index between the horizontal velocities of the separation of opposite polarity poles and the maximum value of magnetic flux.

Khlystova (2011) presented a statistical study the photospheric Doppler velocities in 83 active regions with a total unsigned magnetic flux above  $10^{21} \text{ Mx}$ . A centre to limb dependence of negative Doppler velocities was established, which indicates that the horizontal velocities of plasma outflows are higher than the vertical upflow velocities during the first hours of the emergence of active regions.

In this article we study the statistical relations between Doppler velocities and magnetic field parameters during the emergence of active regions.

## 2. Data Analysis

We used full-disc SOHO/MDI data (Scherrer *et al.*, 1995). The temporal resolution of the photospheric magnetograms and Dopplergrams is 1 minute, while that of the continuum is 96 minutes. The spatial resolution of the data is  $4''$ . Magnetograms with a 1.8.2 calibration level were used (Ulrich *et al.*, 2009).

We have cropped a region of emerging magnetic flux from a time sequence of data taking into account its displacement caused by solar rotation. This displacement was calculated by the differential rotation law for photospheric magnetic fields (Snodgrass, 1983) and the cross-correlation analysis of two magnetograms adjacent in time. A precise spatial superposition of the data was achieved by cropping fragments with identical coordinates from simultaneously acquired magnetograms and Dopplergrams. For correct processing of the data, we chose the cropped region in a way that it excluded the area outside the limb. For the Dopplergrams the contribution of solar differential rotation and other factors distorting the Doppler velocity signal were removed by using the technique described in Grigor'ev, Ermakova, and Khlystova (2007).

The sequence of the fragments obtained has been used to calculate the temporal variations of the parameters under study. The calculation area was limited to the region of the emerging magnetic flux. The boundary of emerging flux region was visually inspected.

The total unsigned magnetic flux of active regions was calculated inside isolines  $\pm 60$  G taking into account the projection effect and assuming that the magnetic field vector is perpendicular to the solar surface:

$$\Phi = S_0 \sum_{i=1}^N \frac{|B_i|}{\cos \theta_i}, \quad (1)$$

where  $\Phi$  is the total unsigned magnetic flux in Mx,  $S_0$  is the area of the solar surface of pixel in the centre of solar disc in  $cm^2$ ,  $N$  is the number of pixels where  $|B_i| > 60$  G,  $B_i$  is the line of sight magnetic field strength of  $i$ th pixel in G,  $\theta_i$  is the heliocentric angle of  $i$ th pixel. The maximum total unsigned magnetic flux  $\Phi_{max}$  was determined by the maximum inflection point in the increase of the magnetic flux curve or by the last value of the datasets (for active regions passing beyond the west limb or with insufficiently downloaded data). The signal background that existed before the emergence of active regions was subtracted from the maximum total unsigned magnetic flux. Magnetic saturation in measurements of the magnetic field strength in SOHO/MDI was controlled (Liu, Norton, and Scherrer, 2007); it was attained only in three of the active regions considered.

The total unsigned magnetic flux growth rate  $d\Phi/dt$  and absolute value of the maximum magnetic field strength  $H_{max}$  were calculated in the first 12 hours of the emergence of the magnetic flux for large and small active regions or from beginning to maximum of the total unsigned magnetic flux for ephemeral active regions.

Photospheric plasma flows are characterised by the peak (absolute maximum) values of negative and positive Doppler velocities  $V_{max-}$  and  $V_{max+}$  which were

determined in the first 12 hours of the magnetic flux emergence for large and small active regions or from beginning to maximum of the total unsigned magnetic flux for ephemeral active regions. The magnetic flux emergence begins with the appearance of the loop apex where the magnetic field is horizontal; therefore, the time interval we analysed started 30 minutes before the appearance of the line of sight magnetic fields. Continuum images were used to control the possible formation of sunspots with Evershed flows in the first hours of the emergence of active regions to eliminate their contribution. The maximum Doppler velocity of these flows in SOHO/MDI data with low spatial resolution can reach  $2 \text{ km s}^{-1}$  (Bai, Scherrer, and Bogart, 1998).

The position of the active region on the solar disc is expressed by the heliocentric angle  $\theta$ :

$$\theta = \arcsin(r/R), \quad (2)$$

where  $r$  is the distance from the disc centre to the place of the active region emergence and  $R$  is the solar radius.  $\theta$  is also approximately the angle between the normal to the surface and the line of sight component of the emerging magnetic flux.

We performed a regression analysis of the data. There is at least one inflection point in the considered dependencies. Therefore, linear or quadratic polynomials were used as approximation functions. The choice of the polynomial degree was based on the minimum values of the standard deviations. The results are given in the form of polynomial equations which, according to the F-statistic, are significant. The confidence intervals for the means were calculated with a confidence probability of 99%.

### 3. The Investigated Active Regions

We have studied 224 active regions which emerged on the visible side of the solar disc from 1999 to 2008 (see Figure 1). The selected active regions have different spatial scales and emerge at different distances from the solar disc centre. They are isolated from high concentrations of existing magnetic fields (the presence of single poles with total unsigned magnetic flux not higher than  $0.5 \times 10^{21} \text{ Mx}$  in the region of the direct emergence of the active region for the first hours was allowed). Sufficiently complete data series with a temporal resolution of 1 minute for the first hours of magnetic flux emergence are available for the selected objects.

The statistical analysis includes the following.

1. According to the maximum value of the total unsigned magnetic flux (in the two polarities):
  - 68 ephemeral active regions ( $2.6 \times 10^{18} \text{ Mx} < \Phi_{max} < 4.07 \times 10^{20} \text{ Mx}$ );
  - 130 small active regions ( $4.07 \times 10^{20} \text{ Mx} < \Phi_{max} < 8 \times 10^{21} \text{ Mx}$ );
  - 26 large active regions ( $\Phi_{max} > 8 \times 10^{21} \text{ Mx}$ ).

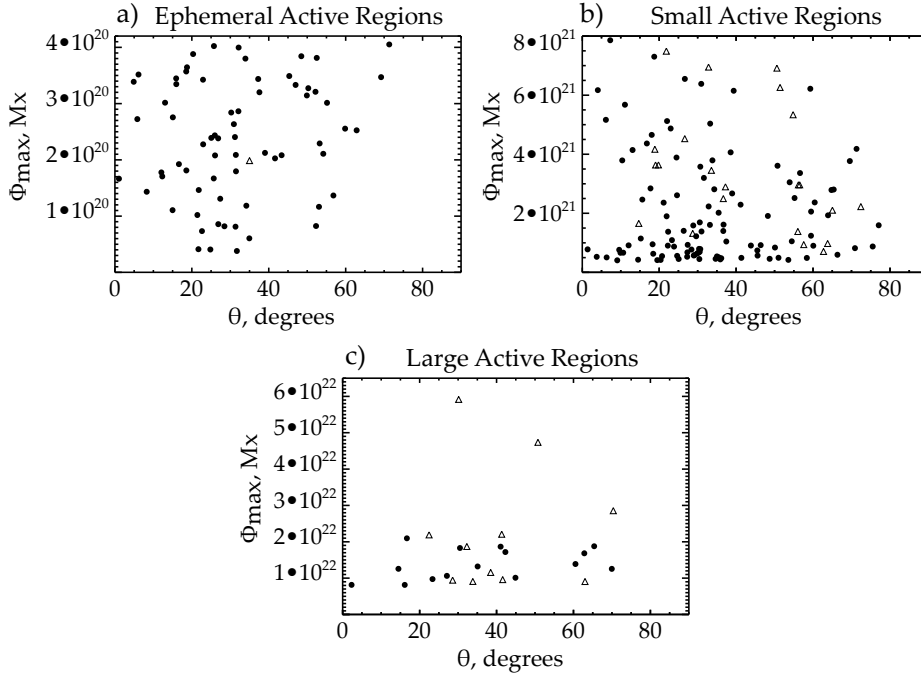


**Figure 1.** Maximum total unsigned magnetic flux of the (a) ephemeral, (b) small and (c) large active regions versus the heliocentric angle that corresponds to the beginning of the emergence of magnetic fluxes. The total magnetic flux maximum was determined by the maximum inflection point in the increase of the magnetic flux curve (marked by points) or by the last measurement (marked by triangles). Active regions with magnetic saturation are also marked by triangles. In active regions marked by triangles, the maximum of the total unsigned magnetic flux may be higher.

The limits of the total unsigned magnetic flux for ephemeral active regions were taken from Hagenaar (2001). The limit between the large and small active regions is considered to be the maximum magnetic flux in one polarity; it is taken equal to  $5 \times 10^{21}$  Mx (Garcia de La Rosa, 1984; Zwaan, 1987). In the present investigation the limit between the large and small active regions was chosen at the total unsigned magnetic flux in two polarities, equal to  $8 \times 10^{21}$  Mx, since all active regions with the total unsigned magnetic flux above this level contain sunspots and their spatial size exceeds the size of a supergranule.

2. According to the distances from the solar disc centre:

- 72 active regions near the solar disc centre ( $\theta < 25^\circ$ );
- 98 active regions at medium distance from disc centre ( $25^\circ < \theta < 50^\circ$ );
- 54 active regions near the limb ( $\theta > 50^\circ$ ).

The maximum Doppler velocities of the convection flow in the quiet Sun were calculated at different distances from the disc centre using SOHO/MDI data (Figure 2). Dopplergrams with 1 minute temporal resolution for the period 18–23 April 2001 were used. The peak values of negative and positive Doppler

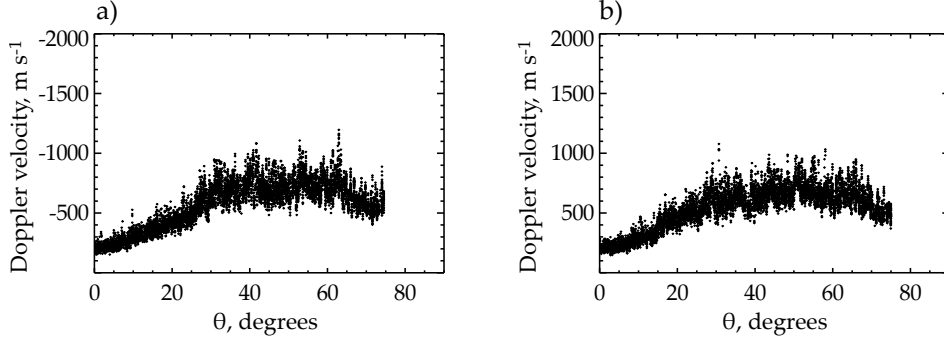


**Figure 2.** Peak (a) negative and (b) positive Doppler velocities of the convective flows in the quiet Sun versus the heliocentric angle for SOHO/MDI data.

velocities were measured within a region of size  $40'' \times 40''$  whose displacement was tracked based on the differential rotation law of Doppler structures in the photosphere (Snodgrass and Ulrich, 1990). The selected region was going through the W00–W75 range of longitudes along the equator during the period under study. The contribution of solar differential rotation and other factors distorting the Doppler velocity signal were removed by using the technique described by Grigor'ev, Ermakova, and Khlystova (2007).

In Figure 2 one observes that Doppler velocities of convection flows increases with the heliocentric angle. For the points with  $\theta > 60^\circ$  there is a tendency for Doppler velocities to decrease. This may be due to the Doppler velocities being measured in higher atmospheric layers near the limb, due to the increase in the optical thickness, where the atmosphere is convectively stable and convection flows are damped.

## 4. Results

### 4.1. The Centre to Limb Dependence of Negative Doppler Velocities

The peak values of negative Doppler velocities (plasma motion toward the observer) in the first hours of magnetic flux emergence of ephemeral, small and large active regions show an increase with the heliocentric angle (Figure 3). The regression analysis of the data yielded Equations (3) for ephemeral, (4) for small, and (5) for large active regions:

$$V_{max-} = -211.32 - 24.77\theta + 0.16\theta^2, \quad (3)$$

$$V_{max-} = -134.93 - 33.05\theta + 0.26\theta^2, \quad (4)$$

$$V_{max-} = -96.35 - 34.75\theta + 0.22\theta^2, \quad (5)$$

where  $V_{max-}$  is the peak negative Doppler velocity in  $\text{m s}^{-1}$  and  $\theta$  is the heliocentric angle in degrees that corresponds to the position of the region at  $V_{max-}$ .

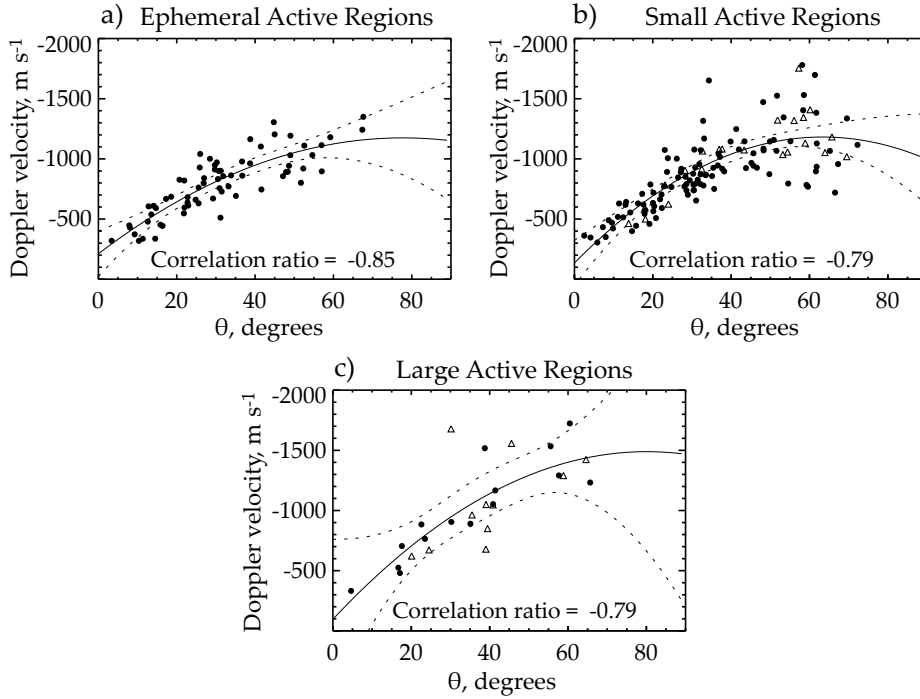


**Figure 3.** Peak negative Doppler velocities (plasma motion towards the observer) in the first hours of the emergence of (a) ephemeral, (b) small and (c) large active regions versus the heliocentric angle that corresponds to the position of the region at this time. The solid line corresponds to Equations (3) in plot (a), (4) in plot (b) and (5) in plot (c); dotted lines correspond to 99% confidence intervals for the means.

Correlation ratios show a strong relation between the considered parameters:  $-0.85$  for ephemeral,  $-0.79$  for small and  $-0.79$  for large active regions. The dependencies obtained indicate that during the emergence of active regions the horizontal velocities of plasma outflows ( $\theta > 50^\circ$ ) exceed the vertical upflow velocities ( $\theta < 25^\circ$ ). Generally, the Doppler velocities accompanying the emergence of active regions are higher than those of convective flows, however, sometimes they are comparable. For small and large active regions the horizontal Doppler velocity component substantially exceeds horizontal Doppler velocities of the convection flows in the quiet Sun, which are less than  $1200 \text{ m s}^{-1}$  (Figure 3 b, c, and Figure 2 a the points with  $\theta > 50^\circ$ ).

#### 4.2. Vertical Doppler Velocities

For the active regions emerging near the solar disc centre ( $\theta < 25^\circ$ ), peak negative Doppler velocities (plasma upflow) have a high dispersion and correlate neither with the magnetic flux growth rate (the correlation ratio is  $-0.30$ ) nor with the maximum magnetic field strength (the correlation ratio is  $-0.22$ ) (Figure 4). The dependencies obtained imply that the upflow Doppler velocities do not characterise the power of the emerging magnetic flux.

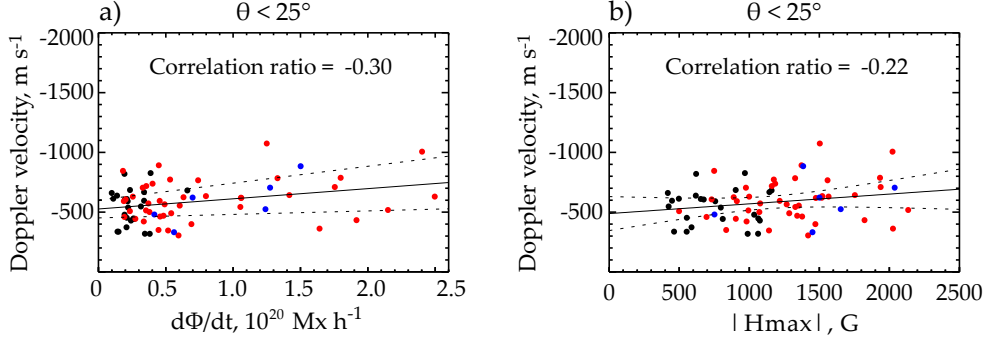


**Figure 4.** Peak negative Doppler velocities (plasma motion toward the observer) versus (a) the magnetic flux growth rate and (b) the maximum magnetic field strength in the first hours of the emergence of active regions near the solar disc centre ( $\theta < 25^\circ$ ). Black symbols are for ephemeral active regions, red symbols for small active regions and blue symbols for large active regions.

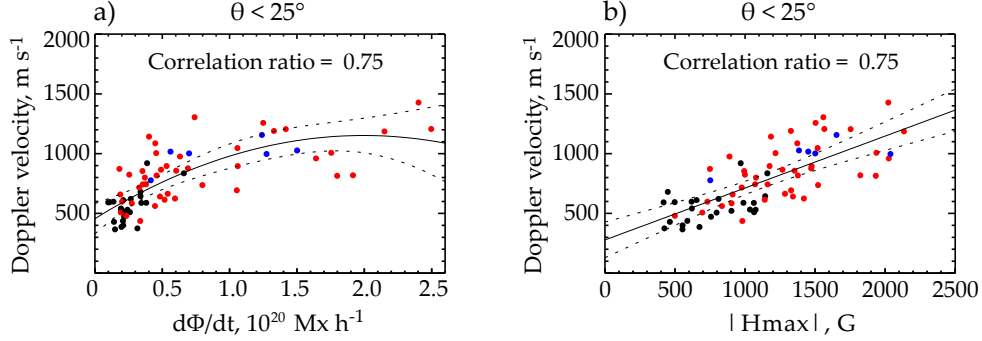


**Figure 5.** Peak positive Doppler velocities (plasma motion away from the observer) versus (a) the magnetic flux growth rate and (b) the maximum magnetic field strength in the first hours of the emergence of active regions near the solar disc centre ( $\theta < 25^\circ$ ). The solid line corresponds to Equations (6) in plot (a) and (7) in plot (b); dotted lines correspond to 99% confidence intervals for the means. The symbol colours are the same as in Figure 4.

For the active regions emerging in the central part of the solar disc ( $\theta < 25^\circ$ ), the peak positive Doppler velocities (plasma downflow) are related quadratically to the magnetic flux growth rate (the correlation ratio is 0.75) and linearly with the maximum magnetic field strength (the correlation ratio is 0.75) (Figure 5). The linear dependence shown on Figure 5 b confirms the results obtained previously by Bonaccini *et al.* (1991), Keil *et al.* (1999), Grigor'ev, Ermakova, and Khlystova (2011). The Doppler velocity values substantially exceed convection Doppler velocities in the quiet Sun (Figure 5 and Figure 2 b the points with  $\theta < 25^\circ$ ).

Regression analysis of the data yielded the following equations:

$$V_{max+} = 455.82 + 6.98 \times 10^{-18} d\Phi/dt - 1.75 \times 10^{-38} (d\Phi/dt)^2, \quad (6)$$

$$V_{max+} = 277.94 + 0.43 \times H_{max}, \quad (7)$$



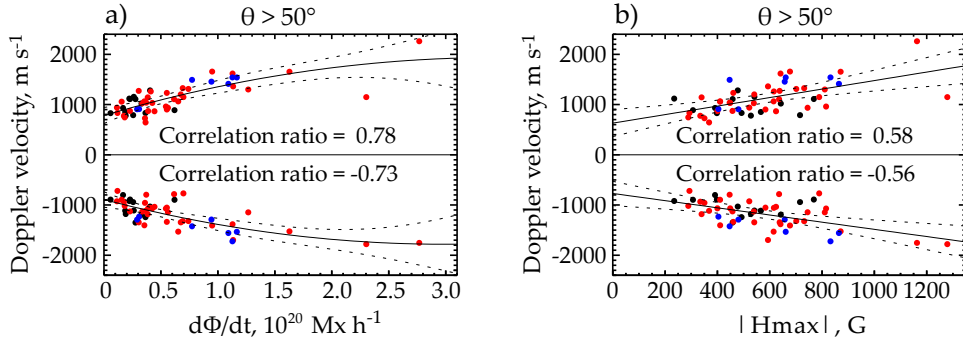


**Figure 6.** The peak positive and negative Doppler velocities versus (a) the magnetic flux growth rate and (b) maximum magnetic field strength in the first hours of the emergence of active regions near the limb ( $\theta > 50^\circ$ ). The solid line corresponds to Equations (8) and (9) in plot (a) and Equations (10) and (11) in plot (b), dotted lines correspond to 99% confidence intervals for the means. The symbol colours are the same as in Figure 4.

where  $V_{\text{max}+}$  is the peak positive Doppler velocity in  $\text{m s}^{-1}$ ,  $d\Phi/dt$  is the magnetic flux growth rate in  $\text{Mx h}^{-1}$  and  $H_{\text{max}}$  is the maximum magnetic field strength in G.

The draining of the cold plasma, being carried out by the emerging magnetic flux from the convective zone into the solar atmosphere, is considered to be the main reason for the plasma observed downflows.

#### 4.3. Horizontal Doppler Velocity

Khlystova (2012) has carried out a detailed analysis of photospheric flows in four active regions emerging near the solar limb. It has been found that extended regions of Doppler velocities with different signs are formed in the first hours of the magnetic flux emergence in the horizontal velocity field. The observed Doppler velocities substantially exceed the separation velocities of the photospheric magnetic flux outer boundaries and most likely are caused by the significant component of the velocities of plasma downflow being carried out into the solar atmosphere by emerging magnetic flux.

One observes in Figure 3 that the horizontal Doppler velocity component ( $\theta > 50^\circ$ ) in the region of emerging magnetic fluxes has a wide range of values. For the active regions emerging near the limb ( $\theta > 50^\circ$ ), the peak positive and negative Doppler velocities of photospheric plasma flows show a quadratic relation with the magnetic flux growth rate (correlation ratios 0.78 and  $-0.73$ ) and a linear relation with the maximum magnetic field strength (correlation ratios 0.58 and  $-0.56$ ) (Figure 6). Strong magnetic fields are oriented mainly perpendicular to the surface after the emergence. Therefore, the magnetic field strength in active regions near the limb is 2–3 times smaller than that one in active regions near the solar disc centre, because of the projection effects of the magnetic field vector to the line of sight (Figure 6 b and Figure 5 b).

Regression analysis of the data yielded the following equations:

$$V_{\text{max}+} = 782.27 + 6.68 \times 10^{-18} d\Phi/dt - 9.65 \times 10^{-39} (d\Phi/dt)^2, \quad (8)$$

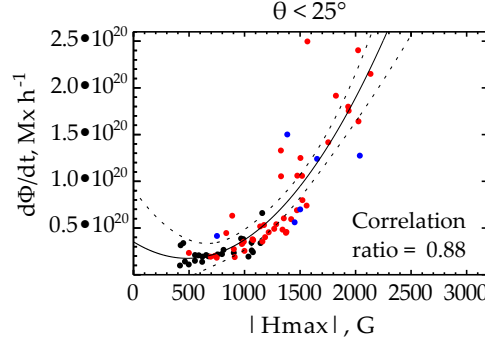


**Figure 7.** Magnetic flux growth rate versus the magnetic field strength in the first hours of the emergence of active regions near the solar disc centre ( $\theta < 25^\circ$ ). The solid line corresponds to Equation (12); dotted lines correspond to 99% confidence intervals for the means. The symbol colours are the same as in Figure 4.

$$V_{max-} = -890.85 - 5.95 \times 10^{-18} d\Phi/dt + 9.94 \times 10^{-39} (d\Phi/dt)^2, \quad (9)$$

$$V_{max+} = 630.53 + 0.85 \times H_{max}, \quad (10)$$

$$V_{max-} = -770.35 - 0.71 \times H_{max}, \quad (11)$$

where  $V_{max+}$  and  $V_{max-}$  are, respectively, the peak values of positive and negative Doppler velocities in  $\text{ms}^{-1}$ ,  $d\Phi/dt$  is the magnetic flux growth rate in  $\text{Mx h}^{-1}$  and  $H_{max}$  is the maximum magnetic field strength in G.

One sees in Figure 5a and Figure 6a that the horizontal Doppler velocities exceed the vertical downflow Doppler velocities by a factor of 1.5–2 in the active regions with the same magnetic flux growth rate. This supports theoretical models in which the velocities of draining plasma have a significant horizontal component at the beginning of the magnetic flux emergence (see Shibata *et al.* (1990), Archontis *et al.* (2004), Toriumi and Yokoyama (2010), Toriumi *et al.* (2011) and others).

#### 4.4. The Relation between the Magnetic Flux Growth Rate and the Maximum Strength of Magnetic Fields

A quadratic relation with relatively low dispersion and a high correlation ratio of 0.88 between the magnetic flux growth rate and the density of the magnetic fields for the active regions emerging near the solar disc centre ( $\theta < 25^\circ$ ) has been found (Figure 7). The equation derived by the regression analysis has the following form:

$$d\Phi/dt = 3.52 \times 10^{19} - 7.27 \times 10^{16} H_{max} + 7.49 \times 10^{13} H_{max}^2, \quad (12)$$

where  $d\Phi/dt$  is the magnetic flux growth rate in the first hours of the emergence in  $\text{Mx h}^{-1}$  and  $H_{max}$  is the maximum magnetic field strength in G.

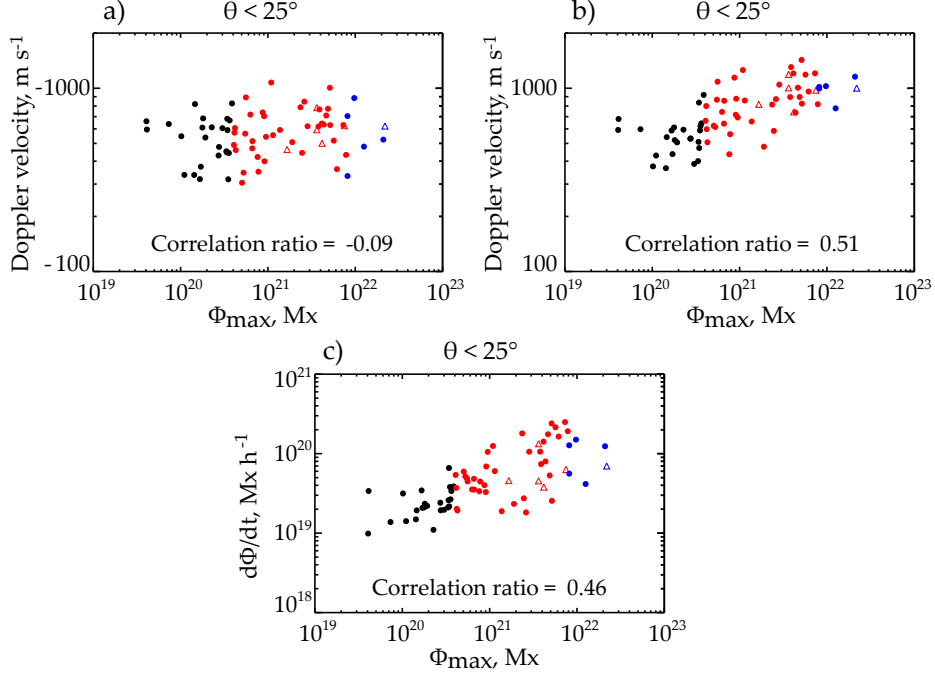


**Figure 8.** The relation between (a) peak negative Doppler velocities, (b) peak positive Doppler velocities and (c) the magnetic flux growth rate in the first hours of the emergence of active regions with total unsigned magnetic flux at the maximum of their development  $\Phi_{\max}$ . The symbol colours are the same as in Figure 4. The  $\Phi_{\max}$  was determined by the maximum inflection point in the increase of the flux curve (marked by points) or by the last measurement (marked by triangles). In active regions marked by triangles, the  $\Phi_{\max}$  may be higher.

The dependence is theoretically expectable. The magnetic flux emerge due to the action of the magnetic buoyant force which is proportional to the square of the magnetic field density  $B^2$  (Parker, 1955). The higher the magnetic field strength, the higher the magnetic pressure and the lower the gas pressure inside the magnetic structure. The low gas pressure leads to a large magnetic buoyancy force and, thus, to an increase in the magnetic flux growth rate.

#### 4.5. The Relation of Parameters between the Beginning and Maximum Development of Active Regions

Active regions emerging near the solar disc centre ( $\theta < 25^\circ$ ) are considered. Peak negative Doppler velocities in the first hours of the magnetic flux emergence do not show any relation with the total unsigned magnetic flux at maximum development of the active regions (Figure 8 a). Comparison of the peak positive Doppler velocities and the magnetic flux growth rate with the maximum value of total unsigned magnetic flux reveals a power-law relation with high dispersion (Figure 8 b, c). A power-law relation, but with less dispersion, between the flux growth rate and the the maximum value of magnetic flux has been found earlier by Otsuji *et al.* (2011). In the present investigation the weak dependence between

the parameters under consideration can be explained by the fact that active region magnetic flux emerges in separate fragments on time scales from several hours to 5–7 days. Therefore, the parameters of magnetic fields and Doppler velocities in the first hours of emergence do not characterise an active region as a whole.

## 5. Conclusions

The study of plasma flow Doppler velocities and magnetic field parameters during the emergence of active regions at the photospheric level has revealed the following statistical relationships:

1. Peak values of negative Doppler velocities accompanying the magnetic flux emergence in the first hours show an increase with the heliocentric angle  $\theta$ . The observed relation shows that horizontal velocities of plasma outflows are higher than the vertical upflow velocities.
2. The upflow plasma Doppler velocities have no relation with parameters of magnetic fields and, thus, do not characterise the power of the emerging magnetic flux.
3. The downflow plasma Doppler velocities have high values, which substantially exceed Doppler velocities of convection flows in the quiet Sun. They are related quadratically with the magnetic flux growth rate and linearly with the maximum magnetic field strength. The main reason for the observed downflows is considered to be a draining of the cold plasma, being carried out into the solar atmosphere by the emerging magnetic flux.
4. The horizontal plasma outflow Doppler velocities are connected quadratically with the magnetic flux growth rate and linearly with the maximum magnetic field strength. Possibly the horizontal flows are connected with draining of plasma which has a significant horizontal component at the beginning of the magnetic flux emergence.
5. There is a quadratic dependence with relatively low dispersion and a high correlation ratio of 0.88 between the magnetic flux growth rate and the maximum strength of magnetic fields. The observed relation is consistent with the magnetic buoyancy law.
6. There is a weak power-law dependence of peak positive Doppler velocities and the magnetic flux growth rate in the first hours of the emergence of active regions with the maximum value of the total unsigned magnetic flux.

**Acknowledgements** The author is grateful to the referee for helpful comments that improved the manuscript. The author thanks V. M. Grigor'ev, L. V. Ermakova and V. G. Fainshstein for useful discussions. This work used data obtained by the SOHO/MDI instrument. SOHO is a mission of international cooperation between ESA and NASA. The MDI is a project of the Stanford-Lockheed Institute for Space Research. This study was supported by RFBR grants 10-02-00607-a, 10-02-00960-a, 11-02-00333-a, 12-02-00170-a, the state contracts of the Ministry of Education and Science of the Russian Federation No. 02.740.11.0576, 16.518.11.7065, the program of the Division of Physical Sciences of the Russian Academy of Sciences No. 16, the Integration Project of SB RAS No. 13 and the program of Presidium of Russian Academy of Sciences No. 22.

## References

- Archontis, V., Moreno-Insertis, F., Galsgaard, K., Hood, A., O'Shea, E.: 2004, Emergence of magnetic flux from the convection zone into the corona. *Astron. Astrophys.* **426**, 1047–1063. doi:10.1051/0004-6361:20035934.
- Bachmann, G.: 1978, On the evolution of magnetic and velocity fields of an originating sunspot group. *Bulletin of the Astronomical Institutes of Czechoslovakia* **29**, 180–184.
- Bai, T., Scherrer, P.H., Bogart, R.S.: 1998, The Evershed Effect: an MDI Investigation. In: S. Korzennik (ed.) *Structure and Dynamics of the Interior of the Sun and Sun-like Stars*, *ESA Special Publication* **418**, 607–610.
- Barth, C.S., Livi, S.H.B.: 1990, Magnetic Bipoles in Emerging Flux Regions on the Sun. *Rev. Mex. Astron. Astrofis.* **21**, 549–551.
- Bonaccini, D., Landi Degl'Innocenti, E., Smaldone, L.A., Tamblyn, P.: 1991, High resolution spectropolarimetry of an active region. In: L. J. November (ed.) *Solar Polarimetry*, 251–256.
- Brants, J.J.: 1985a, High-resolution spectroscopy of active regions. II Line-profile interpretation, applied to an emerging flux region. *Solar Phys.* **95**, 15–36. doi:10.1007/BF00162633.
- Brants, J.J.: 1985b, High-resolution spectroscopy of active regions. III - Relations between the intensity, velocity, and magnetic structure in an emerging flux region. *Solar Phys.* **98**, 197–217. doi:10.1007/BF00152456.
- Brants, J.J., Steenbeek, J.C.M.: 1985, Morphological evolution of an emerging flux region. *Solar Phys.* **96**, 229–252. doi:10.1007/BF00149682.
- Cho, K.-S., Bong, S.-C., Chae, J., Kim, Y.-H., Park, Y.-D.: 2010, Tiny Pores Observed by Hinode/Solar Optical Telescope. *Astrophys. J.* **723**, 440–448. doi:10.1088/0004-637X/723/1/440.
- Chou, D., Wang, H.: 1987, The separation velocity of emerging magnetic flux. *Solar Phys.* **110**, 81–99. doi:10.1007/BF00148204.
- Frazier, E.N.: 1972, The Magnetic Structure of Arch Filament Systems. *Solar Phys.* **26**, 130–141. doi:10.1007/BF00155113.
- Garcia de La Rosa, J.I.: 1984, The observation of intrinsically different emergences for large and small active regions. *Solar Phys.* **92**, 161–172. doi:10.1007/BF00157243.
- Golovko, A.A.: 1998, Relationship between the maximum magnetic fluxes and lifetimes of solar active regions. *Astron. Rep.* **42**, 546–552.
- Gopasyuk, S.I.: 1967, The velocity field in an active region at spot appearance stage. *Izvestiya Ordena Trudovogo Krasnogo Znameni Krymskoj Astrofizicheskoy Observatorii* **37**, 29–43.
- Gopasyuk, S.I.: 1969, The velocity field on the two levels in the active region of July 1966. *Izvestiya Ordena Trudovogo Krasnogo Znameni Krymskoj Astrofizicheskoy Observatorii* **40**, 111–126.
- Grigor'ev, V.M., Ermakova, L.V., Khlystova, A.I.: 2007, Dynamics of line-of-sight velocities and magnetic field in the solar photosphere during the formation of the large active region NOAA 10488. *Astronomy Letters* **33**, 766–770. doi:10.1134/S1063773707110072.
- Grigor'ev, V.M., Ermakova, L.V., Khlystova, A.I.: 2009, Emergence of magnetic flux at the solar surface and the origin of active regions. *Astron. Rep.* **53**, 869–878. doi:10.1134/S1063772909090108.
- Grigor'ev, V.M., Ermakova, L.V., Khlystova, A.I.: 2011, The dynamics of photospheric line-of-sight velocities in emerging active regions. *Astron. Rep.* **55**, 163–173. doi:10.1134/S1063772911020041.
- Guglielmino, S.L., Martínez Pillet, V., Ruiz Cobo, B., Zuccarello, F., Lites, B.W.: 2006, A Detailed Analysis of an Ephemeral Region. *Memorie della Societa Astronomica Italiana Supplementi* **9**, 103–105.
- Hagenaar, H.J.: 2001, Ephemeral Regions on a Sequence of Full-Disk Michelson Doppler Imager Magnetograms. *Astrophys. J.* **555**, 448–461. doi:10.1086/321448.
- Harvey, K.L., Martin, S.F.: 1973, Ephemeral Active Regions. *Solar Phys.* **32**, 389–402. doi:10.1007/BF00154951.
- Kawaguchi, I., Kitai, R.: 1976, The velocity field associated with the birth of sunspots. *Solar Phys.* **46**, 125–135. doi:10.1007/BF00157559.
- Keil, S.L., Balasubramaniam, K.S., Smaldone, L.A., Reger, B.: 1999, Velocities in Solar Pores. *Astrophys. J.* **510**, 422–443. doi:10.1086/306549.
- Khlystova, A.: 2011, Center-limb dependence of photospheric velocities in regions of emerging magnetic fields on the Sun. *Astron. Astrophys.* **528**, A7. doi:10.1051/0004-6361/201015765.

- Khlystova, A.: 2012, The Horizontal Component of Photospheric Plasma Flows During the Emergence of Active Regions on the Sun. *Solar Phys.*, in *Topical Issue "Advances of European Solar Physics"*. doi:10.1007/s11207-012-0181-8.
- Kubo, M., Shimizu, T., Lites, B.W.: 2003, The Evolution of Vector Magnetic Fields in an Emerging Flux Region. *Astrophys. J.* **595**, 465–482. doi:10.1086/377333.
- Lagg, A., Woch, J., Solanki, S.K., Krupp, N.: 2007, Supersonic downflows in the vicinity of a growing pore. Evidence of unresolved magnetic fine structure at chromospheric heights. *Astron. Astrophys.* **462**, 1147–1155. doi:10.1051/0004-6361:20054700.
- Lites, B.W., Skumanich, A., Martinez Pillet, V.: 1998, Vector magnetic fields of emerging solar flux. I. Properties at the site of emergence. *Astron. Astrophys.* **333**, 1053–1068.
- Liu, Y., Norton, A.A., Scherrer, P.H.: 2007, A Note on Saturation Seen in the MDI/SOHO Magnetograms. *Solar Phys.* **241**, 185–193. doi:10.1007/s11207-007-0296-5.
- Otsuji, K., Kitai, R., Ichimoto, K., Shibata, K.: 2011, Statistical Study on the Nature of Solar-Flux Emergence. *Pub. Astron. Soc. Japan* **63**, 1047–1057.
- Parker, E.N.: 1955, The Formation of Sunspots from the Solar Toroidal Field. *Astrophys. J.* **121**, 491–507. doi:10.1086/146010.
- Parnell, C.E., DeForest, C.E., Hagenaar, H.J., Johnston, B.A., Lamb, D.A., Welsch, B.T.: 2009, A Power-Law Distribution of Solar Magnetic Fields Over More Than Five Decades in Flux. *Astrophys. J.* **698**, 75–82. doi:10.1088/0004-637X/698/1/75.
- Scherrer, P.H., Bogart, R.S., Bush, R.I., Hoeksema, J.T., Kosovichev, A.G., Schou, J., Rosenberg, W., Springer, L., Tarbell, T.D., Title, A., Wolfson, C.J., Zayer, I., MDI Engineering Team: 1995, The Solar Oscillations Investigation - Michelson Doppler Imager. *Solar Phys.* **162**, 129–188. doi:10.1007/BF00733429.
- Schoolman, S.A.: 1973, Videomagnetograph Studies of Solar Magnetic Fields. II: Field Changes in an Active Region. *Solar Phys.* **32**, 379–388. doi:10.1007/BF00154950.
- Shibata, K., Nozawa, S., Matsumoto, R., Sterling, A.C., Tajima, T.: 1990, Emergence of solar magnetic flux from the convection zone into the photosphere and chromosphere. *Astrophys. J. Lett.* **351**, L25–L28. doi:10.1086/185671.
- Snodgrass, H.B.: 1983, Magnetic rotation of the solar photosphere. *Astrophys. J.* **270**, 288–299. doi:10.1086/161121.
- Snodgrass, H.B., Ulrich, R.K.: 1990, Rotation of Doppler features in the solar photosphere. *Astrophys. J.* **351**, 309–316. doi:10.1086/168467.
- Solanki, S.K., Lagg, A., Woch, J., Krupp, N., Collados, M.: 2003, Three-dimensional magnetic field topology in a region of solar coronal heating. *Nature* **425**, 692–695. doi:10.1038/nature02035.
- Strous, L.H., Zwaan, C.: 1999, Phenomena in an Emerging Active Region. II. Properties of the Dynamic Small-Scale Structure. *Astrophys. J.* **527**, 435–444. doi:10.1086/308071.
- Tarbell, T.D., Topka, K., Ferguson, S., Frank, Z., Title, A.M.: 1989, High - resolution observations of emerging magnetic flux. In: O. von der Luehe (ed.) *High spatial resolution solar observations*, 506–520.
- Toriumi, S., Yokoyama, T.: 2010, Two-step Emergence of the Magnetic Flux Sheet from the Solar Convection Zone. *Astrophys. J.* **714**, 505–516. doi:10.1088/0004-637X/714/1/505.
- Toriumi, S., Miyagoshi, T., Yokohama, T., Isobe, H., Shibata, K.: 2011, Dependence of the Magnetic Energy of Solar Active Regions on the Twist Intensity of the Initial Flux Tubes. *Pub. Astron. Soc. Japan* **63**, 407–415.
- Ulrich, R.K., Bertello, L., Boyden, J.E., Webster, L.: 2009, Interpretation of Solar Magnetic Field Strength Observations. *Solar Phys.* **255**, 53–78. doi:10.1007/s11207-008-9302-9.
- Xu, Z., Lagg, A., Solanki, S.K.: 2010, Magnetic structures of an emerging flux region in the solar photosphere and chromosphere. *Astron. Astrophys.* **520**, A77. doi:10.1051/0004-6361/200913227.
- Zwaan, C.: 1987, Elements and patterns in the solar magnetic field. *Annual review of astronomy and astrophysics* **25**, 83–111. doi:10.1146/annurev.aa.25.090187.000503.
- Zwaan, C., Brants, J.J., Cram, L.E.: 1985, High-resolution spectroscopy of active regions. I - Observing procedures. *Solar Phys.* **95**, 3–14. doi:10.1007/BF00162632.